JET-P(96)15

Spectroscopic Investigation of C IV

M Tunklev[1], L Engström[1], C Jupén[1], I Kink[1],
I Martinson[1], A Meigs.

JET Joint Undertaking, Abingdon, Oxfordshire, OX14 3EA, UK.
[1] Department of Physics, University of Lund, Sweden.

Preprint of a paper to be submitted for application in
Physics Scripts

May 1996

ABSTRACT

This paper reports an investigation of the spectrum and term system of Li-like carbon, C IV. Between 200 and 7750 Å a total of 105 C IV lines have been identified by combining previously known data with new spectra recorded by the beam-foil technique and from observations at the JET tokamak, where pollutions of the charge exchange spectras is an incentive for this C IV investigation. A comprehensive term system, with accurate energies for all levels up to n = 12, is constructed from the identified transitions. Semi-empirical series formulae are also given, allowing reliable extrapolations to still higher n values. The ionization energy is determined to (520176.1 ± 1.5) cm^{-1}.

INTRODUCTION

The method of charge exchange spectroscopy, CXS, has in recent years become a powerful tool for the diagnosis of fusion plasmas [1-4]. This technique of active diagnostics involves the injection of neutral beams, H, D or He (typically of 20 - 50 keV/amu kinetic energy) into the plasma core. Here charge exchange (CX) reactions $A^{q+} + B \rightarrow A^{(q-1)+} + B^{+}$ can occur between the neutral atoms (B) and the stripped low Z impurity ions A^{q+}. As a result of this CX process the impurities are preferentially excited into high n,l states [5] which decay by photon emission, typically in the visible wavelength range. Thus, highly charged elements, the resonance lines of which lie in the XUV, can be observed in more comfortable spectral regions which largely facilitates observations. For instance, measurements of line-widths and line-shifts due to Doppler effects, to determine ion temperatures and toroidal rotational velocities, can be conveniently performed.

Furthermore, diagnostics using spectral features such as He II (n = 3-4) at 4685 Å and C VI (n = 7-8) at 5291 Å can be significantly affected by the passive CX background spectrum originating in the vicinity of the last closed flux surface or magnetic separatrix. This passive CX spectrum is thought to be governed by plasma ions striking the wall and creating neutral deuterium or hydrogen with thermal velocities sufficient to reach the fully stripped ions at the magnetic separatrix [6]. In the present work a number of C IV lines belonging to the 6-8, 7-10 and 8-11 transitions arrays have been identified for the first time in a spectrum from JET. This knowledge may help to reduce some of the ambiguities in CX ion temperature measurements.

In view of the relevance of C for JET we have undertaken a comprehensive spectral analysis of C IV based on the combination of the most accurate data available from previous investigations using different spark sources (reviewed in the next section) and new observations obtained by the beam-foil technique and from plasma spectroscopy at JET. The combination of beam-foil results with those of other techniques takes full advantage of the

merits of the different methods while avoiding some of their drawbacks, and has previously proved to be very effective in generating highly accurate and comprehensive term analyses. Examples closely related to the present work are the investigations of Li-like fluorine, F VII [7] and He-like carbon, C V [8].

Much theoretical interest has also been focussed on the structure of Li-like ions. Theoretical and computational developments in recent years have made it possible to simultaneously handle electron correlation, relativistic and quantum electrodynamic (QED) effects in three-electron systems. Thus, *ab initio* data of spectroscopic accuracy have been reported for the $1s^2nl$ states up to n = 5 for Z = 3 - 11 [9,10] and for the n = 2 states all the way up to Uranium [11]. New, highly accurate experimental results serve as valuable tests of such elaborate calculations.

SURVEY OF PREVIOUS WORK

The first comprehensive study of C IV was reported by Edlén [12] who, using an open spark as light source, classified nearly 60 spectral lines and determined experimental energies for all terms with n < 8. Incidentally, this early work was also of great astrophysical significance because Edlén [13] identified several emission lines in the spectra of hot Wolf-Rayet stars as transitions in C IV. Subsequently Bockasten [14] continued the work on C IV, thereby determining several additional transitions within the term table established by Edlén [12]. However, the light source used by Bockasten was a sliding vacuum spark where the effective ionic field was about 25 kV/cm, and, according to [14], all terms except ns, np (n < 7), 3d, 4d and 4f were more or less affected by Stark shifts. The most recent measurement of the important 2s ^{2}S - 2p ^{2}P resonance lines have been performed by Bockasten *et al.* [15]. This analysis resulted in a significant change (0.017 Å) in the $^2S_{1/2}$ - $^2P_{3/2}$ wavelength compared to the value given in [14], while confirming the 1/2 - 1/2 transition. The new 1/2 - 3/2 value is also in much better agreement with the result obtained by Edlén [12].

Perevertun and Mukhtarov [16] recorded C IV spectra in the grazing-incidence region around 200 Å and determined some additional ns, np and nd terms with n up to 14. In the early 1970's beam-foil spectroscopy was also used to study C IV, which resulted in some new level determinations [17,18]. However, the wavelength accuracy quoted in these beam-foil studies is quite modest by present day standards, and not sufficient for high quality spectroscopy.

While these previous experimental studies have provided valuable material for C IV, additional work is still well motivated. Thus, the spectral region 700 - 2000 Å has not been thoroughly explored. Furthermore, the high-lying nl levels should be investigated by means of light sources that both strongly populate such states and avoid interionic electric fields. The beam-foil excitation fulfills these requirements. The population mechanism closely resembles

the charge exchange processes which, in a more clear-cut way, are observed in ion-atom collisions, and leads to a copious production of states with high n and l quantum numbers. Moreover, the very low particle density in the ion beam results in negligible interionic fields which eliminates Stark shifts completely.

EXPERIMENT

Intense beams of C ions were obtained from the 3 MV Pelletron tandem accelerator at Lund. The ions were accelerated to 1.5, 2.5 or 3 MeV energy and directed through a thin carbon foil. The optimum energy for the production of C^{3+} is around 1.5 MeV. But the additional energies allowed us to make charge state classifications of the observed lines by studying their relative intensities as a function of energy. Furthermore, at the higher energies all C II and all but the most intense C III lines have disappeared, leaving a cleaner spectrum of only C IV and C V lines. The light emitted by the foil-excited ions was analyzed with a Minuteman 310 NIV 1 m normal incidence vacuum monochromator, which can be equipped with a number of interchangeable concave gratings. The present work is based on spectra recorded in the 600 - 5000 Å range, using a number of different grating/detector combinations to optimize the experimental conditions. Thus, spectra from 500 to 2700 Å were recorded with a 1200 l/mm grating, blazed at 1500 Å, and a CsI-coated channeltron. This detector provided intense first order lines up to about 1700 Å together with many lines in higher spectral orders. A small section from this spectrum is shown in Figure 1. From this recording C IV lines below 700 Å could be measured in up to the third order whereas lines between 700 and 1200 Å were studied in the first and second spectral orders. The 1100 - 2400 Å interval was also recorded using the same grating but with an EMR 541 photomultiplier equipped with a LiF window, to eliminate possible blends caused by overlapping spectral orders. Typical line-widths (FWHM) in this spectral range are 0.8 Å. Finally, the 2200 - 2600 Å and 4600 - 5300 Å regions (containing n = 4 - 5 and n = 5 - 6 transitions,respectively) were measured at a beam energy of 1.5 MeV using a 600 l/mm grating blazed at 3000 Å and a Hamamatsu R 585 photomultiplier. In this case the typical line-widths are 1.5 and 2 Å in the two regions, respectively. The increasing FWHM in this case arises because at this comparatively low ion energy the Doppler-broadening caused by the line-of-sight velocity induced by multiple scattering in the foil is not

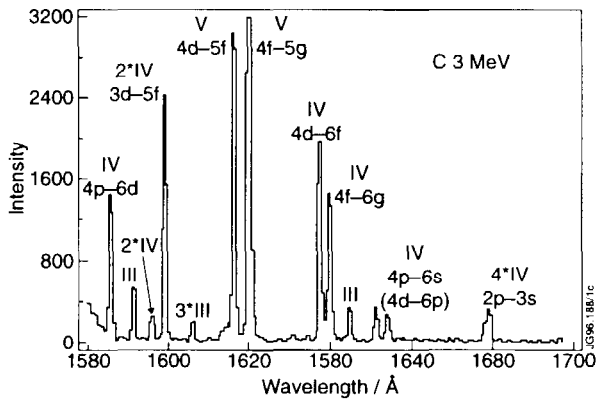

*Fig.1: Part of beam-foil spectrum of C recorded at 3 MeV. The different spectral orders observed are indicated as (spectral order) * (spectral number).*

negligible. Parts of this spectral material have also been used in previous analyses of core-excited levels in C IV [19] and of C V [8].

The JET CX diagnostics are built on a multichord system with line-of-sights intersecting various parts of the plasma core. To measure the ion temperature and bulk rotation of the plasma core, line-of-sights crossing the injected neutral beam in the equatorial magnetic midplane are used to maximize the Doppler effects. The spectra used in this work, however, are obtained along a vertical line of sight intersecting the neutral beam perpendicularly, where no Doppler shifts should affect the measurements. The spectra were recorded by means of the new KT3D spectrometer, equipped with a 300 l/mm grating and imaging around 12 cm of the divertor region. The spectrometer with its CCD detector covers an interval of about 500 Å at each setting between 4000 and 8000 Å, with an observed line width ranging from 1.5 to 4 Å.

ANALYSIS

Wavelength determinations and the experimental term system

To determine the wavelengths of the observed lines we followed a two step procedure. First the peak positions were found using both an automatic peak-finding routine and an interactive program (CARATE [20]) that fits a sum of Gaussians to the observed spectrum. The latter program yields significantly improved results in cases where the spectral features are only partially resolved. In the second step these peak positions were converted to absolute wavelengths using polynomial calibration functions derived from accurately known in-beam reference lines from C III [21], C IV [12,14,15] and C V [8,22]. The weighted averages of the wavelengths determined at the different energies and in different spectral orders are given in Table I. By combining the statistical uncertainty in the peak positions with that from the calibration procedure we estimate that the average uncertainty in the quoted wavelengths for well-resolved lines below 2400 Å is 0.05 Å. This estimate is also consistent with the observed scatter of the individual results around the quoted averages. For the 4d-5f and 4f-5g transitions, which were measured in both first and second orders, we estimate an uncertainty of 0.1 Å, whereas for the lines around 4660 Å an uncertainty of 0.15 Å is obtained. The larger value in this case is due to the larger line-widths observed, as discussed above. The wavelengths obtained from the JET spectra are estimated to have uncertainties between 0.1 and 0.2 Å.

Combining the transitions identified in this work with the previously known material [12,14,15] (Table I) yields a well connected term system. This is illustrated in Figure 2, where most of the terms and transitions established experimentally in C IV are included. The best esti-mates of the energy levels are derived from the observed transitions in a least-squares procedure where each line is weighted by its estimated wavenumber uncertainty. In this fitting

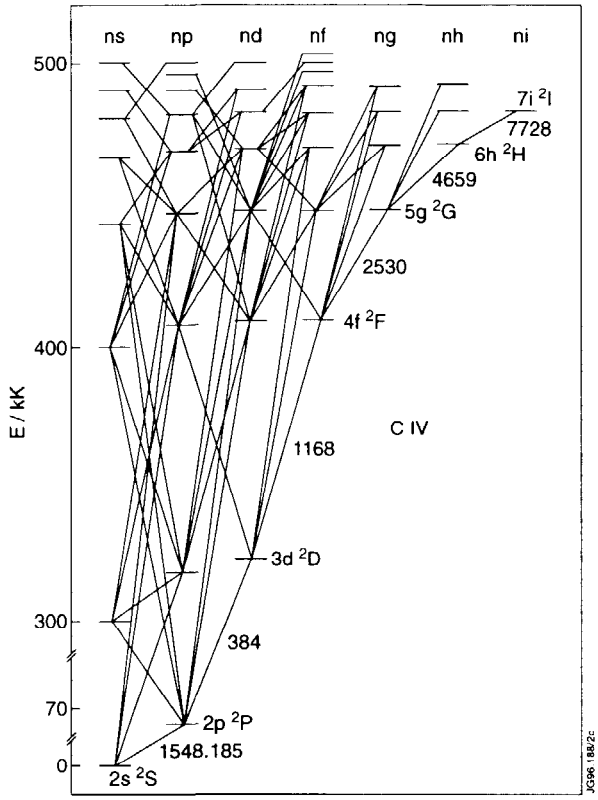

Fig.2: The term system of C IV and most of the obser-ved transitions. Transition wavelengths are given in Å.

process a minor problem arises from the presence of both fine-structure resolved and unresolved trans-itions involving some p and d terms. For example, Edlén [12] found two 3d-4f lines whereas in this work the 3d-5f transition is observed as a single line. To handle this problem we chose to fit only the centre-of-gravity energies of the nd terms, whereas the fine-structure levels were retained for the np terms. To accomplish this, all transitions to fine-structure resolved d-states were recalculated to represent combinations with the centre-of-gravity, while, on the other hand, unresolved transitions involving a p-state were split into two artificial lines corresponding to the two fine-structure levels. In these calculations we used the hydrogenic fine-structure separation for the nd states whereas the np splittings were obtained by scaling the accurate experimental results for 2p according to $\Delta_{(2p)} = \Delta_{(np)}\ (n^*_{2p}/n^*_{np})^3$, where n^* is the effective quantum number. For both np and nd ($n > 3$) states the splittings thus calculated should be more accurate than those derived from the previous experiments.

The resulting level values are given in Table II, which also includes the number of combinations found with a particular level. The column marked "ΔE" in Table II gives a measure of the relative uncertainty in the level value. To estimate the uncertainty in the absolute values of the energies one should add (quadratically) the uncertainty obtained for the ground state which is 1 cm^{-1}. The wavelengths calculated from the fitted energy levels are given in column 3 of Table I. In column 4 of Table I these values are compared to the observed wavelengths, and we find in all cases agreement within the estimated experimental errors.

Series formulae and the ionization energy

In a Li-like ion the outer nl electron moves virtually undisturbed in a field that closely resembles that of a hydrogen-like ion with a nuclear chargeζ = Z-2 (i.e. the two $1s^2$ core-electrons provide an almost perfect shielding of the nucleus). In such cases the deviations between the observed term energies and the exact H-like values, caused by small core-penetration and polarization effects, can be accurately described by the Ritz formalism [23].

$$T = E_{ip} - E_{nl} = R\zeta^2/(n-\delta_l)^2 = R\zeta^2/n^{*2}$$

where T is the term value, E_{ip} the ionisation energy, E_{nl} the experimental excitation energy and δ_l is the so-called quantum defect. δ_l is strongly dependent on the l-quantum number but only weakly on n. In the Ritz formalism δ_l is written as:

$$\delta_l = a + bt + ct^2 + ..., \text{ with } t = T/R\zeta^2.$$

For so-called penetrating orbitals, in this case s and p, three Ritz parameters (a, b and c) were necessary to represent the observed energies within their estimated uncertainties. For the higher l-states two parameters sufficed. From a fit of these implicit relations between E_{nl}, E_{ip} and the Ritz parameters for each Rydberg series (given l) accurate values of the ionization energy may be derived. Applying the Ritz formalism to the centre-of-gravity energies for the C IV doublets results in very consistent ionization energies for the different Rydberg series. We thus obtain E_{ip} = 520176.0, 6.3, 4.4, 4.6 and 7.6 cm^{-1} for the ns to ng series, respectively. However, for the nf and ng series the quantum defect is very small, leading to large uncertainties in the fitted parameters. Furthermore, for these series an erroneous slope of the quantum defect vs. n curves is obtained. Thus, as our final value of the ionization energy we adopt the weighted average from the ns, np and nd series of E_{ip} = (520176.1 ± 1.5) cm^{-1}. The quoted error estimate takes into account also the uncertainty of about 1 cm^{-1} in the absolute energy values, mentioned above. The new value of the limit confirms the previous result of 520177.0 cm^{-1} [14].

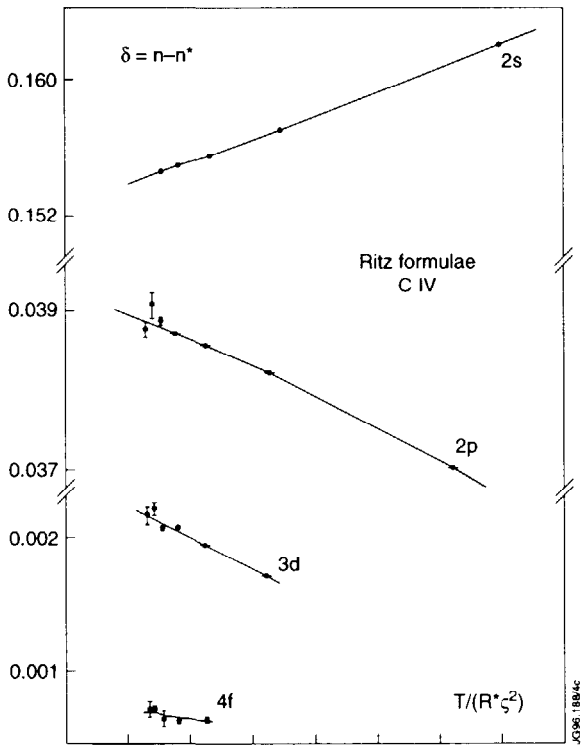

Fig.3: The observed quantum defect as a function of reduced term value for the s-f Rydberg series. The curves represent the fitted Ritz formule with the ionisation energy held constant at the adopted value for all series.

Using the adopted value of the ionisation energy as a constant new Ritz formulae were derived for the s to f series. For this value of the ionization energy we find that the quantum defect in the nf terms display the correct n-dependence. These fits are illustrated in Figure 3 and the Ritz parameters obtained are given in Table III. The difference between the experimental excitation energy and that calculated from the Ritz formulae is given in the last column in Table II. As the n-value increases along a

Rydberg series the orbitals become more and more hydro-genic, hence the Ritz formulae may be used to accurately extrapolate the observed series to higher n-values. Extrapolated energies up to n = 12 are included in Table II. In particular the short-wavelength resonance transitions 2s ^{2}S - np ^{2}P calculated from these energy values should be considerably more reliable than the experimental data [12,16] and may, in fact, be useful as wavelength standards.

For so-called non-penetrating orbitals (l > 1 in a Li-like ion) the quantum defect is mainly caused by the polarization of the core in the field of the outer electron. In this case the polarization parameterization [23] may be used to describe theterm values of allnon-penetrating nl-orbitals using only two constants, α_d and α_q, representing the dipole- and quadrupole polarizability of the core. A fit of these parameters and the ionization energy to the nd, nf and ng series in C IV is illustrated in Figure 4. This type of plot is the standard way to represent the polarization formula graphically. (For the definition of the variables in Figure 4 we refer to [23]). The ionization limit obtained in this way is 520176.0 ± 0.3 cm^{-1}, in perfect agreement with the results discussed above from the Ritz procedure. For the polarizabilities we obtain $\alpha_d = (9.16 \pm 0.5)\cdot 10^{-3}$ a_o^3 and $\alpha_q = (1.13 \pm 0.1)\cdot 10^{-3}$ a_o^5, which may be compared to the isoelectronic predictions of Edlén [24] giving $\alpha_d = 8.882\cdot 10^{-3}$ a_o^3 and $\alpha_q = 1.227\cdot 10^{-3}$ a_o^5. Table II includes extrapolated level energies for the nf and ng series up to n = 12 based on the fitted polarization parameters.

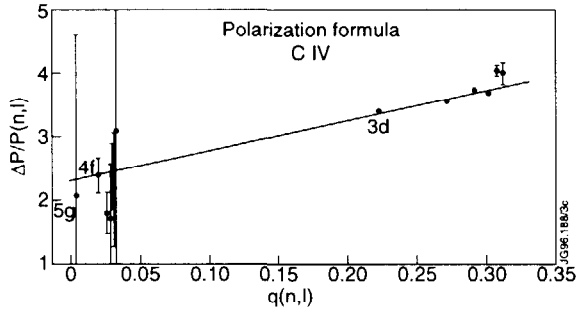

Fig.4: The polarization formula [23] fitted to the non-penetrating nd-ng series in C IV.

CONCLUSIONS

This investigation of C IV contains all spectral transitions expected to be found in most lightsources, including the JET tokamak. It is therefore now possible to reveal and find previously unknown blends and components in all atomic spectras from the various diagnostic groups at JET.

ACKNOWLEDGEMENTS

We are grateful to Dr. M. von Hellermann for valuable discussions. Three of the authors (MT, CJ, IM) acknowledge the hospitality extended to them at JET. This work has been supported by the Swedish Natural Science Research Council (NFR).

REFERENCES

1. A. Boileau, M. von Hellermann, L.D. Horton, J. Spencer and H.P. Summers, Plasma Phys. Contr. Fusion **31**, 779 (1989).
2 M. von Hellermann, W. Mandl, H.P. Summers, A. Boileau, R. Hoekstra, F.J. de Heer and J. Frieling, Plasma Phys. Contr. Fusion 33, 1805 (1991).
3. R.C. Isler, Plasma Phys. Contr. Fusion 36, 171 (1994).
4. R. Hoekstra, Comments Atom. Molec. Phys. 30, 361 (1995).
5. M. Mattioli, N.J. Peacook, H.P. Summers, B. Denne and N.C. Hawkes, J. Physique Coll. C1, 329 (1989).
6. M. von Hellermann, and H.P. Summers, "Atomic and Plasma-Material Interaction Processes in Controlled Thermonuclear Fusion", R.K. Janev and H.W. Drawin editors, Elsevier Science Publishers 135 (1993).
7. L. Engström, Physica Scripta 29, 113 (1984).
8. L. Engström, P. Bengtsson, C. Jupén and M. Westerlind, J. Phys. B 25, 2459 (1992).
9. K.T.Chung, Phys. Rev. A 44, 5421 (1991).
10. Z.-W. Wang, X.-W. Zhu and K.T. Chung, Phys. Rev. A 46, 6914 (1992).
11. M.H. Chen, K.T. Cheng, W.R. Johnson and J. Sapirstein, Phys. Rev. A 52, 266 (1995).
12. B. Edlén, Nova Acta Reg. Soc. Sci. Ups. 9, No. 6 (1934).
13. B. Edlén, Z. Astrophysik 7, 378 (1933).
14. K. Bockasten, Arkiv Fysik 10, 567 (1956).
15. K. Bockasten, R. Hallin and T.P. Hughes, Proc. Phys. Soc. 81, 522 (1963).
16. V.M. Perevertun and S.M. Mukhtarov, Opt. Spectrosc. 26, 50 (1969).
17. M.C. Poulizac, M. Druetta and P. Ceyzeriat, J. Quant. Spectrosc. Radiat. Transfer 11, 1087 (1971).
18. M.C. Poulizac and J.P. Buchet, Physica Scripta 4, 191 (1971).
19. L. Engström, R. Hutton, N. Reistad, I. Martinson S. Huldt, S. Mannervik, and E. Träbert, Physica Scripta 36, 250 (1987).
20. L.Carlén, Internal Report LUNFD 6 (NFFK - 7014), University of Lund, (1982).
21. K. Bockasten, Arkiv Fysik 9, 457 (1955).
22. B. Edlén and B. Löfstrand, J. Phys. B 3, 1380 (1970).
23. B. Edlén, in Handbuch der Physik 27, ed. S. Flügge, Springer, Berlin (1964) p. 80.
24. B. Edlén, Physica Scripta 19, 255 (1979).
25. B. Edlén, Rep. Prog. Phys. 26, 181 (1963).

Table 1: Observed C IV transitions.

I^a	λ_{vac} /Å	λ^b_{calc}/Å	o-c /Å	Transition
0	200.68[c]	200.68	0.00	$2s\ ^2S$ – $9p\ ^2P$
1	203.057[c]	203.055	0.002	$2s\ ^2S$ – $8p\ ^2P$
3	206.641[c]	206.634	0.007	$2s\ ^2S$ – $7p\ ^2P$
5	212.421[c]	212.416	0.005	$2s\ ^2S$ – $6p\ ^2P$
7	222.791[c]	222.787	0.004	$2s\ ^2S$ – $5p\ ^2P$
3	238.200[c]	238.188	0.012	$2p\ ^2P_{1/2}$ – $7d\ ^2D$
3	238.250[c]	238.249	0.001	$2p\ ^2P_{3/2}$ – $7d\ ^2D$
10	244.907[c]	244.908	-0.001	$2s\ ^2S$ – $4p\ ^2P$
4	245.775[c]	245.769	0.006	$2p\ ^2P_{1/2}$ – $6d\ ^2D_{3/2}$
5	245.830[c]	245.833	-0.003	$2p\ ^2P_{3/2}$ – $6d\ ^2D_{5/2}$
0	247.357[c]	247.342	0.015	$2p\ ^2P_{1/2}$ – $6s\ ^2S$
1	247.415[c]	247.408	0.007	$2p\ ^2P_{3/2}$ – $6s\ ^2S$
6	259.471[c]	259.470	0.001	$2p\ ^2P_{1/2}$ – $5d\ ^2D_{3/2}$
7	259.542[c]	259.540	0.002	$2p\ ^2P_{3/2}$ – $5d\ ^2D_{5/2}$
3	262.550[c]	262.549	0.001	$2p\ ^2P_{1/2}$ – $5s\ ^2S$
4	262.624[c]	262.623	0.001	$2p\ ^2P_{3/2}$ – $5s\ ^2S$
9	289.143[c]	289.141	0.002	$2p\ ^2P_{1/2}$ – $4d\ ^2D_{3/2}$
10	289.230[c]	289.229	0.001	$2p\ ^2P_{3/2}$ – $4d\ ^2D_{5/2}$
6	296.857[c]	296.857	0.000	$2p\ ^2P_{1/2}$ – $4s\ ^2S$
7	296.951[c]	296.951	0.000	$2p\ ^2P_{3/2}$ – $4s\ ^2S$
10	312.422[d]	312.422	0.000	$2s\ ^2S$ – $3p\ ^2P_{3/2}$
5	312.453[d]	312.452	0.001	$2s\ ^2S$ – $3p\ ^2P_{1/2}$
20	384.032[c]	384.030	0.002	$2p\ ^2P_{1/2}$ – $3d\ ^2D_{3/2}$
10	384.178[c]	384.177	0.001	$2p\ ^2P_{3/2}$ – $3d\ ^2D_{5/2}$
3	419.525[c]	419.526	-0.001	$2p\ ^2P_{1/2}$ – $3s\ ^2S$
6	419.714[c]	419.715	-0.001	$2p\ ^2P_{3/2}$ – $3s\ ^2S$
500	595.53 {	595.49		$3s\ ^2S$ – $6p\ ^2P$
		595.75		$3d\ ^2D$ – $8f\ ^2F$
120	627.12	627.12	0.00	$3d\ ^2D$ – $7f\ ^2F$
600	660.87	660.94	0.07	$3p\ ^2P$ – $6d\ ^2D$
2200	682.51	682.51	0.00	$3d\ ^2D$ – $6f\ ^2F$
1400	684.89	684.88	0.01	$3s\ ^2S$ – $5p\ ^2P$
2200	770.31	770.32	-0.01	$3p\ ^2P$ – $5d\ ^2D$
300	798.09	798.11	-0.02	$3p\ ^2P$ – $5s\ ^2S$
2200	799.63	799.63	0.00	$3d\ ^2D$ – $5f\ ^2F$
1	948.098[c]	948.101	-0.003	$3s\ ^2S$ – $4p\ ^2P_{3/2}$
0	948.214[c]	948.219	-0.005	$3s\ ^2S$ – $4p\ ^2P_{1/2}$
1	1107.600[c]	1107.596	0.004	$3p\ ^2P_{1/2}$ – $4d\ ^2D_{3/2}$
2	1107.933[c]	1107.936	-0.003	$3p\ ^2P_{3/2}$ – $4d\ ^2D_{5/2}$
3	1168.873[c]	1168.882	-0.009	$3d\ ^2D_{3/2}$ – $4f\ ^2F_{5/2}$
4	1168.990[c]	1168.981	0.009	$3d\ ^2D_{5/2}$ – $4f\ ^2F_{7/2}$
100	1184.76	1184.71	0.05	$4p\ ^2P$ – $8d\ ^2D$
1600	1198.58	1198.56	0.02	$3d\ ^2D$ – $4p\ ^2P$

I[a]		λ_{vac} /Å	λ^{b}_{calc}/Å	o-c /Å	Transition		
160		1210.50	1210.65	-0.15	$4s\ ^2S$	–	$7p\ ^2P$
20		1213.64	1213.53	0.11	$4d\ ^2D$	–	$8f\ ^2F$
50		1214.89	1214.89	0.00	$4f\ ^2F$	–	$8g\ ^2G$
2		1230.046[c]	1230.047	-0.001	$3p\ ^2P_{1/2}$	–	$4s\ ^2S$
3		1230.511[c]	1230.525	-0.014	$3p\ ^2P_{3/2}$	–	$4s\ ^2S$
890		1315.73	1315.74	-0.01	$4p\ ^2P$	–	$7d\ ^2D$
3000		1351.24	1351.26	-0.02	$4d\ ^2D$	–	$7f\ ^2F$
2000		1352.93	1352.92	0.01	$4f\ ^2F$	–	$7g\ ^2G$
470		1358.55	1358.51	0.04	$4d\ ^2D$	–	$7p\ ^2P$
500		1440.31	1440.32	-0.01	$4s\ ^2S$	–	$6p\ ^2P$
10		1548.202[e]	1548.202	0.000	$2s\ ^2S$	–	$2p\ ^2P_{3/2}$
10		1550.774[e]	1550.778	-0.004	$2s\ ^2S$	–	$2p\ ^2P_{1/2}$
1400		1585.94	1585.97	-0.03	$4p\ ^2P$	–	$6d\ ^2D$
2000		1637.55	1637.58	-0.03	$4d\ ^2D$	–	$6f\ ^2F$
1800		1640.03	1640.04	-0.01	$4f\ ^2F$	–	$6g\ ^2G$
90	bl C IV	1653.79	1653.84	-0.05	$4p\ ^2P$	–	$6s\ ^2S$
15		1792.82			$5d\ ^2D$	–	$11f\ ^2F$
10		1794.53			$5fg$	–	$11gh$
45		2057.12			$5d\ ^2D$	–	$9f\ ^2F$
70		2059.45			$5fg$	–	$9gh$
30		2065.07		0.00	$5d\ ^2D$	–	$9p\ ^2P$
2		2104.61[f]	2104.61	-0.00	$4s\ ^2S$	–	$5p\ ^2P_{3/2}$
1		2104.91[f]	2104.92	-0.01	$4s\ ^2S$	–	$5p\ ^2P_{1/2}$
16		2122.49	2122.58	-0.09	$5s\ ^2S$	–	$8p\ ^2P$
90		2333.57	2333.50	0.07	$5d\ ^2D$	–	$8f\ ^2F$
130		2336.44			$5fg$	–	$8gh$
340		2405.19	2405.19	0.00	$4p\ ^2P_{1/2}$	–	$5d\ ^2D_{3/2}$
760		2405.84	2405.83	0.01	$4p\ ^2P_{3/2}$	–	$5d\ ^2D_{5/2}$
2000		2524.96	2524.96	0.00	$4d\ ^2D$	–	$5f\ ^2F$
2500		2530.77			$4f\ ^2F$	–	$5g\ ^2G$
2		2534.53[f]	2534.52	0.01	$4f\ ^2F$	–	$5d\ ^2D$
4		2595.86[f]	2595.86	0.00	$4d\ ^2D_{5/2}$	–	$5p\ ^2P_{3/2}$
3		2596.07[f]	2596.07	0.00	$4d\ ^2D_{3/2}$	–	$5p\ ^2P_{1/2}$
4	bl C III	2698.53[f]	2698.54	-0.01	$4p\ ^2P_{1/2}$	–	$5s\ ^2S$
4		2699.50[f]	2699.50	0.00	$4p\ ^2P_{3/2}$	–	$5s\ ^2S$
400		2902.44	2902.32	0.12	$5d\ ^2D$	–	$7f\ ^2F$
600		2906.84			$5fg$	–	$7gh$
1		2935.98[f]	2935.98	-0.00	$5d\ ^2D$	–	$7p\ ^2P$
0		2954.3[f]			$5p\ ^2P_{1/2}$	–	$7s\ ^2S$
1		2954.81[f]			$5p\ ^2P_{3/2}$	–	$7s\ ^2S$
2		3935.41[f]	3935.31	0.1	$5s\ ^2S$	–	$6p\ ^2P_{3/2}$
1		3936.00[f]	3935.90	0.1	$5s\ ^2S$	–	$6p\ ^2P_{1/2}$
80		4441.45	4441.40	0.05	$5p\ ^2P_{1/2}$	–	$6d\ ^2D_{3/2}$
170		4442.51	4442.56	-0.05	$5p\ ^2P_{3/2}$	–	$6d\ ^2D_{5/2}$

I^a		λ_{vac} /Å	λ^b_{calc}/Å	o-c /Å	Transition		
35		4555.64[g]	4555.66	-0.02	*6p* ^2P	–	*8d* ^2D
200	bl C III	4647.95	4647.78	0.17	*5d* ^2D	–	*6f* ^2F
400		4659.48			*5fg*	–	*6gh*
160		4679.31[g]	4679.34	-0.03	*6d* ^2D	–	*8f* ^2F
50		4686.32			*6fgh*	–	*8ghi*
160		4737.57[g]	4737.56	0.01	*6d* ^2D	–	*8p* ^2P
380		4787.23[g]	4787.29	-0.05	*5d* ^2D	–	*6p* ^2P
70		4790.70[g]			*6p* ^2P	–	*8s* ^2S
1		5017.97[f]	5017.99	-0.02	*5p* $^2P_{1/2}$	–	*6s* ^2S
2		5019.79[f]	5019.77	0.02	*5p* $^2P_{3/2}$	–	*6s* ^2S
25		5056.17[g]			*7s* ^2S	–	*10p* ^2P
35		5358.55[g]			*7p* ^2P	–	*10d* ^2D
55		5465.94[g]			*7d* ^2D	–	*10f* ^2F
20		5520.24[g]			*7p* ^2P	–	*10s* ^2S
10		5802.94[f]	5802.95	-0.01	*3s* ^2S	–	*3p* $^2P_{3/2}$
9		5813.59[f]	5813.59	0.00	*3s* ^2S	–	*3p* $^2P_{1/2}$
500		7382.92[g]	7382.97	-0.05	*6p* ^2P	–	*7d* ^2D
300		7709.13[g]	7709.15	-0.02	*6d* ^2D	–	*7f* ^2F
3800		7727.92[g]			*6fgh*	–	*7ghi*

a: Intensities should onlybe compared for closelyseparated lines. Lines observed in this work have intensities in a linear scale, whereas lines from previous works are given in a logarithmic scale.

b: Wavelength calculated from the experimental level energies given in Table 2. The difference (o-c) between observed and calculated value is omitted if a level is based on only one transition.

c: Edlén[12]

d: Edlén[25]

e: Bockasten[15]

f: Bockasten[14]

g: Observed at JET

Table 2: Energy levels in C IV.

Level	Energy [a] /cm^{-1}	ΔE[b] /cm^{-1}	N[c]	o-c[d] /cm^{-1}
$2s\ ^2S$	0.0	0.0	12	0.0
$3s\ ^2S$	302847.8	0.2	8	0.0
$4s\ ^2S$	401346.5	0.6	9	0.8
$5s\ ^2S$	445365.7	0.5	9	-0.6
$6s\ ^2S$	468782.5	0.2	6	0.1
$7s\ ^2S$	482704.0	1.2	1	-0.6
$8s\ ^2S$	491649.1	0.7	1	-0.4
$9s\ ^2S$	497735.6[e]			
$10s\ ^2S$	502062.0	1.3	1	-0.9
$11s\ ^2S$	505249.4[e]			
$12s\ ^2S$	507663.4[e]			
$2p\ ^2P_{1/2}$	64483.8	0.5	10	0.0
$2p\ ^2P_{3/2}$	64591.0	0.5	10	
$3p\ ^2P_{1/2}$	320048.9	0.2	7	0.0
$3p\ ^2P_{3/2}$	320080.4	0.2	7	
$4p\ ^2P_{1/2}$	408308.6	0.6	9	-0.4
$4p\ ^2P_{3/2}$	408321.8	0.5	9	
$5p\ ^2P_{1/2}$	448854.2	0.2	6	0.3
$5p\ ^2P_{3/2}$	448861.2	0.2	6	
$6p\ ^2P_{1/2}$	470772.8	0.5	6	-1.0
$6p\ ^2P_{3/2}$	470776.6	0.5	6	
$7p\ ^2P$	483946.9	1.3	4	-1.8
$8p\ ^2P$	492478.2	0.5	3	0.7
$9p\ ^2P$	498314.2[e]			
$10p\ ^2P$	502481.8	1.2	1	-1.3
$11p\ ^2P$	505564.1[e]			
$12p\ ^2P$	507905.1[e]			
$3d\ ^2D_{3/2}$	324878.5	0.8	6	-0.7
$3d\ ^2D_{5/2}$	324887.7	0.8	6	
$4d\ ^2D_{3/2}$	410334.4	0.4	8	1.0
$4d\ ^2D_{5/2}$	410338.3	0.4	8	
$5d\ ^2D_{3/2}$	449885.5	0.5	11	-1.0
$5d\ ^2D_{5/2}$	449887.5	0.5	11	
$6d\ ^2D_{3/2}$	471369.6	0.3	6	0.0
$6d\ ^2D_{5/2}$	471370.8	0.3	6	
$7d\ ^2D$	484320.0	0.5	6	-2.0
$8d\ ^2D$	492726.1	0.6	4	-1.2
$9d\ ^2D$	498489.5[e]			
$10d\ ^2D$	502608.7	1.3	1	-2.1
$11d\ ^2D$	505659.9[e]			
$12d\ ^2D$	507978.9[e]			

Level	Energy [a] /cm^{-1}	ΔE[b] /cm^{-1}	N[c]	o-c[d] /cm^{-1}
4f ^2F	410431.5	1.1	5	-0.2
5f ^2F	449941.3	0.7	5	1.2
6f ^2F	471402.4	1.2	3	0.8
7f ^2F	484341.9	0.4	4	-0.2
8f ^2F	492740.8	0.5	3	-0.1
9f ^2F	498499.1[e]			
10f ^2F	502617.8[e]			
11f ^2F	505665.2[e]			
12f ^2F	507983.0[e]			
5g ^2G	449945.2	1.9	1	-0.2
6g ^2G	471405.8	0.9	2	1.1
7g ^2G	484345.6	1.3	2	1.4
8g ^2G	492743.8	1.9	2	1.4
9g ^2G	498500.1[e]			
10g ^2G	502618.6[e]			
11g ^2G	505665.8[e]			
12g ^2G	507983.4[e]			

a: Fine structure splittings in the *np* series are given as $\Delta_{np}=\Delta_{2p}(n^*_{2p}/n^*_{np})^3$, whereas in the *nd* series the hydrogenic values are used.

b: Relative uncertainty. An absolute error estimate is obtained by adding 1 cm^{-1} , corresponding to the uncertainty in the ground level.

c: Number of combinations.

d: Difference between the observed energy value and that calculated from the semi-empirical series formulae. For the *ns* and the center-of-gravity of the *np* and *nd* series the Ritz formalism is used whereas for the *nf* and *ng* series we have applied the polarization formula.

e: Extrapolated value from the series formulae (as defined in footnote d).

Table 3: Ritz formulae for the ns, np, nd and nf series in C IV

		a	b	c
ns	^2S	1.5442(-1)[a]	2.5281(-2)	1.0380(-2)
np	^2P	3.8512(-2)	-4.6344(-3)	-4.9364(-3)
nd	^2D	2.4057(-3)	-6.9973(-3)	
nf	^2F	3.1463(-4)	-1.5976(-3)	

$\delta = a + bt + ct^2$, $\delta = n - n^*$, $t = T/R\zeta^2$. Ionization energy: 520 176.1 cm^{-1}. a: x(y) implies $x \times 10^y$.